Pulsed Field Magnetization of a Rectangular Y-Ba-Cu-O Bulk, Single Grain Superconductor Assembly

Yuchen Wang [1], Mark D Ainslie [2], Difan Zhou [*1], Yibing Zhang [1], Chuanbing Cai [1], John H Durrell [3], David A Cardwell [3]

[1] Shanghai Key Laboratory of High Temperature Superconductors, Department of Physics, Shanghai University, Shangda Road 99, 200444 Shanghai, China

[2] Department of Engineering, King's College London, London WC2R 2LS, United Kingdom

[3] Department of Engineering, University of Cambridge, Cambridge CB2 1PZ, United Kingdom

[*] Corresponding author

E-mail: dz286@shu.edu.cn

ABSTRACT

The practical magnetization of arrays of multiple single grain, bulk high temperature superconductors (HTSs) is essential for practical applications, such as trapped flux rotating machines, magnetic resonance imaging (MRI) and nuclear magnetic resonance (NMR). We report a systematic investigation of the pulsed field magnetization (PFM) of a bulk assembly consisting of two rectangular Y-Ba-Cu-O (YBCO) bulk single grains, in close proximity, at various temperatures. The measurements of the dynamic variation of the magnetic flux density, supported by numerical analysis, reveal that the induced screening currents during the rise of a pulsed field may greatly enhance the flux density in the region of the junction leading to uneven flux penetration and to an increased likelihood of flux jumps in this region. Such coupling between field and current promotes magnetic flux penetration and improves the peak trapped field from 3.01 T for a bulk single grain to 3.11 T for the bulk assembly at 30 K, improving the magnetization efficiency from 80% to 90%. The peak trapped field was further enhanced to 3.39 T and 3.31 T for the single bulk single grain and the bulk assembly, respectively, by employing a two-step multi-pulse PFM process.

Keywords: Flux jumps, high-temperature superconductors, magnetic flux propagation, trapped field magnets

1. Introduction

Melt-grown, single grain (RE)-Ba-Cu-O bulk superconductors [(RE)BCO, where RE = rare earth element or Y] have long been recognized for their ability to act as powerful trapped field magnets (TFM). Indeed, these technologically important materials can generate significantly higher magnetic flux densities than traditional permanent magnets such as Nd–Fe–B. For example, a trapped field up to 17.6 T has been achieved in a stack of two silver-doped GdBCO superconducting bulk samples at 26 K [1]. Murakami *et al*. had previously fabricated a GdBCO bulk superconductor, 65 mm in diameter, whose maximum trapped magnetic field was over 3 T at 77 K [2]. To achieve the maximum tapped field, the bulk superconductors were magnetized by a field cooling magnetization (FCM) technique, which is acknowledged as a standard method to fully magnetize bulk superconductors [3]. However, FCM requires access to a high-field, superconducting DC magnet in general, and is a long-time quasi-static magnetization process, making it impractical for various engineering applications. Pulsed field magnetization (PFM), on the other hand, is a more practical magnetization technique possessing advantages of economy, ease of integration and relatively short magnetization times. Consequently, PFM of bulk, single grain superconductors is

being investigated widely [4-7].

PFM was recognized to require an applied field, B_a, several times stronger than the target trapped field to overcome the pinning force necessary to drive the magnetic flux into the superconductor [8-10]. A consequence of such dramatic flux motion is to generate heat in the sample, thus suppressing the critical current density, J_c, and reducing the trapped field [11, 12]. However, in 2006, Fujishiro *et al*. reported a record-high PFM trapped field of 5.2 T achieved from an applied field of only 6.7 T though a sophisticated multi-pulse magnetization process [13]. Several groups have subsequently observed similar phenomenon. Weinstein *et al*., for example, reported a trapped field of 4.54 T for $B_a = 4.5$ T at 49.1 K, indicating a magnetization efficiency of almost 100% [14].

It has been observed that flux jumps initiated by disturbances in electromagnetic field and temperature [15, 16] may breakdown temporarily the shielding current allowing magnetic flux to penetrate into the superconductor with little hindrance. At the same time, the establishment of a new equilibrium traps the 'jumped' magnetic flux in the body of the superconductor and the whole process is essentially a form of quasi-field cooling [17-20]. Based on this insight, Ainslie *et al*. proposed that "flux jump assisted PFM" could be a widely applicable method for magnetizing single grain bulk superconductors efficiently with a considerably reduced applied magnetic field[21]. Zhou *et al*. further reported that, for a particular sample, there is a threshold B_a required to trigger a flux jump at each operating temperature, B_j [22]. With this characteristic defined, they successfully trapped a magnetic field of up to 4.8 T in a GdBCO bulk single grain using PFM with stable and repeatable results [23]. The magnetic field pattern in real time may be visualized partly by magneto-optical imaging [24, 25] where magnetic flux penetrates into the superconductor in an avalanche in the form of branches [22, 26]. It is notable that the position of the magnetic flux jump is not uniform and is related largely to the uniformity of the sample [27].

The application of bulk single grain superconductors in machines is invariably associated with their ability to trap and/or shield a permeating magnetic field. Although trapped field and integrated flux increase proportionally with sample size, due to challenges in manufacturing large bulk single grains (> 60 mm diameter), it is very difficult to further enhance the trapped field of a bulk superconductor in this way. As an alternative to pursuing the fabrication of larger individual bulk single grains, the use of a bulk assembly could be an effective way of enhancing the total magnetic flux in a practical sample arrangement. Compared with cylindrical bulk geometries, it is considerably easier to form a compact array from rectangular bulk superconductors that is much better suited to a wide variety of devices, including flywheels [28], superconducting rotating machines [29, 30] and superconducting maglev [31]. However, the influence of geometry on flux penetration and the trapped field profile in rectangular bulk single grains and their assembly has not yet been investigated in detail. Unlike the more conventional disk-shaped bulk single grains, the distance of the flux intrusion path between the periphery of the bulk and the center of the single grain is not the same at each position in a rectangular sample. This geometry-dependent difference in penetration distance will directly affect the final trapped field profile of the single grain. In addition, the geometry of the rectangular bulk assembly will affect the distribution of the spatial magnetic field, which may also affect the final trapped field profile.

In this study, we have performed PFM on rectangular bulk superconductors. A series of pulses with different amplitudes have been applied to both a single grain bulk superconductor and an assembly of two bulk single grain samples to investigate their effect on the flux penetration and

trapped field profile of the PFM process. In addition, the effect of a two-step, multi-pulse PFM process on the trapped field has also been investigated in an attempt to improve the final trapped field.

2. Experimental details

2.1. Experimental setup

Figure 1(a) shows a photograph of an assembly of two rectangular YBCO bulk single grains (17×20 mm^2 in the ab-plane and 8 mm in thickness along the c-axis) embedded in a copper sample holder. PFM of a single grain HTS sample was also performed where one of the bulk superconductors was replaced by a polytetrafluoroethylene block of the same size, as shown in Figure 1 (b). The YBCO single grain bulk superconductors were fabricated via the top-seeded melt-growth (TSMG) process at the Nonferrous Metals Institute, Beijing, China. The copper sample holder was slotted to limit the generation of eddy currents during the experiment during the application of strong pulsed fields.

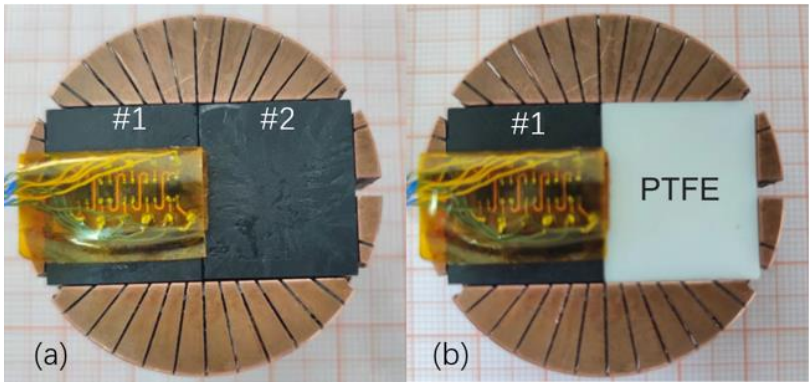

Figure 1. Photographs of (a) an assembly of two rectangular YBCO bulk single grain superconductors and (b) a YBCO bulk single grain with an adjacent polytetrafluoroethylene block.

An FCM experiment was performed using a DC superconducting magnet that could produce a maximum magnetic field of 5 T. Firstly, the bulk sample was cooled in liquid nitrogen in a field of 1 T applied parallel to the *c*-axis. After the sample was thoroughly cooled, the magnetic field was ramped down to 0 T at a rate of 0.18 T min^{-1}. The trapped field profile was then measured directly at the surface of the sample by a scanning Hall sensor system after a relaxation period of 15 minutes to allow the magnetic flux to stabilize. Figure 2 shows that the trapped field profiles of the selected samples (samples #1 and #2) are rather uniform, which indicates their high quality, single grain nature.

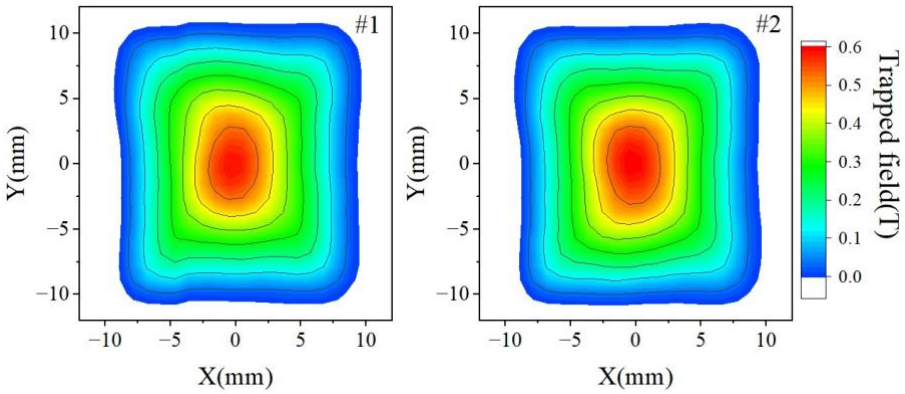

Figure 2. Trapped field profile of sample #1(B_{max}=0.60 T) and sample #2(B_{max}=0.59 T) measured by field cooling magnetization at 77 K.

The PFM experiments were performed using a copper solenoid coil placed outside the vacuum chamber of a GM refrigerator and immersed in liquid nitrogen to reduce the electrical resistance of the coil. The pulsed magnetic field was generated by discharging a capacitor bank through the copper coil. The rise and duration time of the pulsed field was 20 ms and 100 ms, respectively, as shown in Figure 3(a). The peak value can be controlled by adjusting the initial capacitor bank voltage, for which there is a linear relationship. The simulated distribution of the magnetic field in the coil is shown in Figure 3(b). Five Hall sensors were mounted on the surface of the bulk superconductor to measure the trapped flux density and its dynamic variation during the PFM process, as shown in Figure 1. The distance between each adjacent Hall sensor was 2.5 mm. PFM experiments were carried out repeatedly for the single grain bulk sample and the bulk assembly to investigate the influence of the neighboring bulk superconductor on the flux penetration process.

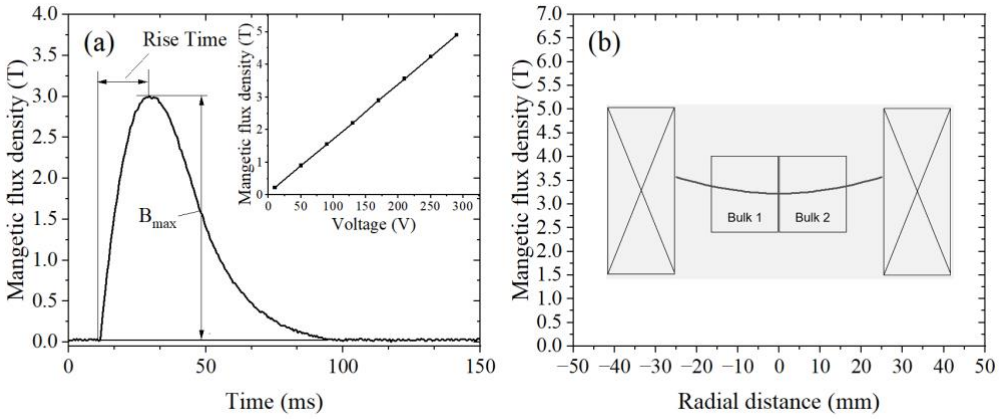

Figure 3. (a) Time dependence of the applied pulsed field at the center of the coil. The inset illustrates the magnetic field at the center of the coil as a function of capacitor bank charging voltage. (b) Amplitude of the radial field following simulation with 200 V applied to the coil.

2.2. Numerical Model

A 3D numerical model based on the H-φ formulation [32] was constructed to obtain a better understanding of the electromagnetic behavior of the single grain sample during the PFM process. The model was implemented using commercial finite element software COMSOL Multiphysics, employing the Magnetic Field Formulation (MFH) and Magnetic Field No Currents (MFNC)

modules, coupled with the Heat Transfer module (HT) for coupling the thermal behaviour. The governing equations for the electromagnetic behaviour are derived from Faraday's and Ampere's laws [33, 34] as follows:

$$\nabla \times \mathbf{H} = \mathbf{J}$$
$$\nabla \times \mathbf{E} = -\frac{\partial \mathbf{B}}{\partial t} \quad (1)$$

The E-J power law is used to simulate the superconductor's non-linear resistivity:

$$\rho_{HTS} = \frac{E_c}{J_c}\left(\frac{J}{J_c(\mathrm{B,T})}\right)^{n-1} \quad (2)$$

where $E_c = 10^{-4}$ V/m and n is a constant set to 21 [35-37]. J_c (B, T) is the magnetic field- and temperature-dependent critical current density and used to define bidirectional coupling of the electromagnetic and thermal physics. It can be can be expressed as:

$$J_c(B,T) = J_{c0} \cdot \frac{(T_c - T)}{(T_c - T_0)} \cdot \frac{B_0}{|B| + B_0} \quad (3)$$

where $T_c = 92$ K is the critical temperature at $B = 0$, and $B_0 = 1.3$ T is constant. A constant value of $J_{c0} = 3.4 \times 10^9$ A/m^2 was used in this study.

The thermal behaviour is based on the following thermal transient equation:

$$\rho \cdot C \frac{dT}{dt} = \nabla \cdot (\kappa \nabla T) + Q \quad (4)$$

where ρ is the mass density, and C and κ are heat capacity and thermal conductivity, respectively. The heat source Q in the conductor is calculated as $Q = \mathbf{E} \cdot \mathbf{J}$ [38-40].

The external magnetic field $B_a(t)$ with a rise time of $\tau = 0.02$ s was approximated using the following equation, where B_{max} is the peak value of B_a. This is applied as a boundary condition on the outer boundaries of the model.

$$B_a(t) = \begin{cases} B_{max} \sin\left(\frac{2\pi t}{0.08}\right) & (t \leqslant 0.02\mathrm{s}) \\ B_{max} e^{\left(\frac{-t}{0.02}+1\right)} & (t > 0.02\mathrm{s}) \end{cases} \quad (5)$$

3. Results and discussion

3.1. Single pulse: single grain bulk sample

Figures 4(a) and (b) show the trapped fields of the bulk single grain after PFM at 70 K and 30 K, respectively. The trapped field profiles were taken 15 minutes after PFM to allow for sufficient relaxation of the trapped magnetic flux. It was found, at 70 K, that the magnetic flux was trapped only at the edges of the sample when the applied field (B_a) was smaller than 2.06 T. Increasing the applied field slightly to $B_a = 2.23$ T increased the peak trapped field abruptly to a maximum of 1.19 T, and was accompanied by a change in the geometry of the trapped field profile from M-shaped to

cone-shaped. Further increase in the applied field only reduced the peak trapped field, which is consistent with existing reports of other PFM studies [41-43]. The dramatic increase in trapped field is attributed to the flux jump phenomenon. Since these are rectangular bulk single grains, the penetration path for the magnetic flux along the longitudinal direction is longer than that along the lateral direction, leading to uneven penetration throughout the sample. It can be observed from Figure 4(a) that the trapped field on the left side of the single grain is slightly higher than that on the right, although the trapped field profile overall is approximately symmetrical.

The effect of the flux jump becomes more pronounced when the temperature is decreased to 30 K due to the increasement of critical current, as shown in Figure 4(b). It can be deduced that the applied field required to trigger a flux jump, defined as B_J, lies between 3.4 T and 3.56 T. The trapped field distribution became noticeably uneven when B_a = 3.56 T was applied. The magnetic flux density at the position of –2.5 mm was significantly higher than that at 2.5 mm. This suggests that the flux jump occurred only in part of the sample.

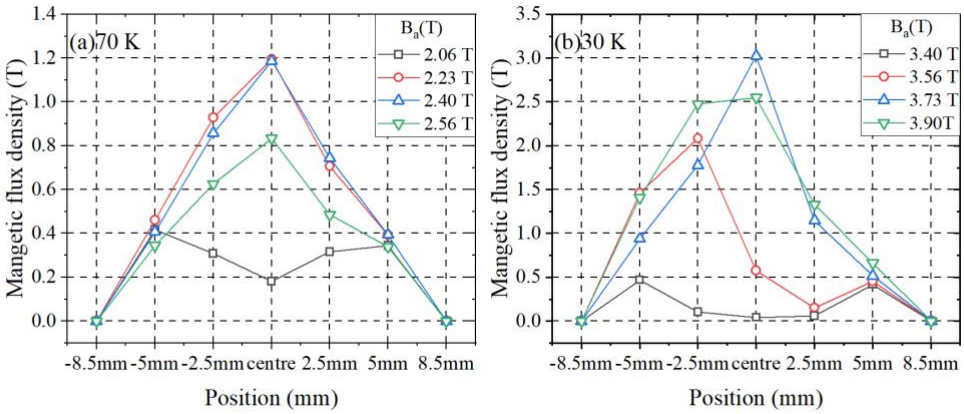

Figure 4. Trapped field profile of the single grain YBCO bulk superconductor for various applied fields B_a at (a) 70 K and (b) 30 K.

Figure 5 shows the dynamic variation of the measured magnetic flux density at different positions within the bulk single grain at 30 K. It is observed that when $B_a(t)$ approached 3.56 T, a sharp rise in the magnetic field occurred suddenly in the left-hand side of the sample at –2.5mm and –5mm. However, the external fields were shielded at positions of 2.5 mm and 5 mm. Therefore, magnetic flux should penetrate into the centre from the left-hand side of the sample.

It is worth mentioning that the sample was placed off-centre inside the coil with its left side closer to the inner edge of the coil [see Figure 3(b)]. The magnetic field at the left edge of the sample is approximately 0.15 T larger than that at the right edge. This explains why the flux jump only occurred in the left part of the sample and provides yet further evidence that the flux jump is very sensitive to the magnitude of the external applied field [7].

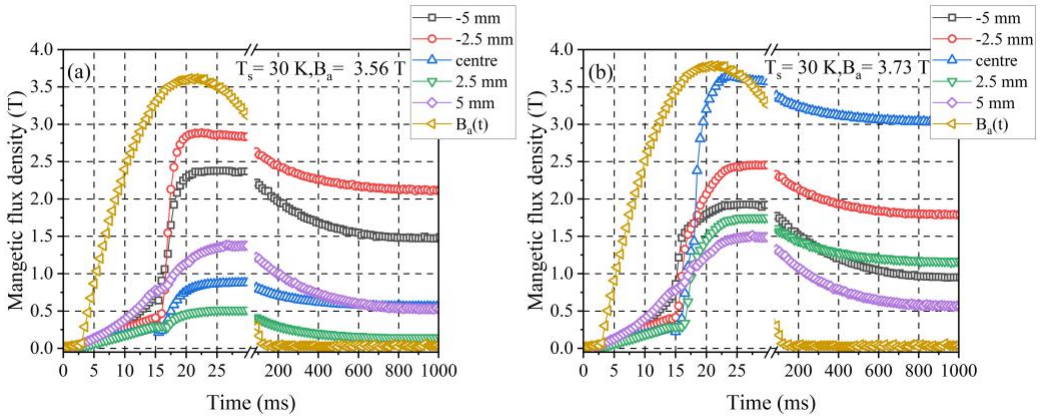

Figure 5. Dynamic variation of the measured magnetic flux density for different positions at 30 K for the single grain YBCO bulk superconductor for (a) B_a = 3.56 T and (b) B_a = 3.73 T.

The PFM experiments were then repeated at temperatures of 60 and 50 K. Figure 6 summaries the dependence of the peak trapped field on the applied magnetic field. In general, as the temperature decreases, a higher applied field is required to fully magnetize the bulk superconductor due to the increased flux pinning ability and therefore J_c. The optimum applied field B_{op} required to achieve the maximum trapped field also increases with decreasing temperature. As the applied magnetic field was increased, the peak trapped field decreased due to the increased heat generated in the bulk single grain. These results are similar to those observed for the individual GdBCO single grain sample in [22]. The maximum trapped field achieved with the single rectangular YBCO single grain at 30 K was 3.02 T for an applied field of 3.73 T. The magnetization efficiency, calculated as B_T/B_a, reached 80%, which is relatively high. It should be noted that the peak trapped field was not always located at the center of the sample and, in some cases, may appear in the vicinity of the centre of the sample as a result of complicated flux motion, especially when flux jumps are involved.

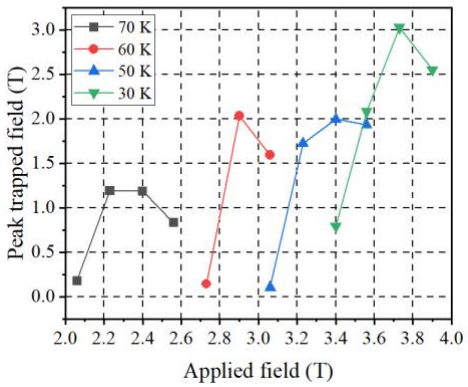

Figure 6. Applied pulsed field B_a dependence of the peak trapped field for the single grain YBCO bulk superconductor at temperatures of 30, 50, 60 and 70 K.

3.2 Single pulse: single grain assembly

The PFM experiments were carried out for the bulk assembly, as shown in Figure 1(b). The same Hall sensor arrangement as that employed for the single grain bulk measurements was used in this experiment. Figure 7 shows the trapped field profiles at 70 K and 30 K, again measured 15 min

after the PFM process. At 70 K, the maximum peak trapped field is 1.10 T when B_a is 2.23 T, which is close to that achieved for the bulk single grain. However, at 30 K, the trapped field distribution is quite different. It can be observed that when B_a is less than 3.56 T, the trapped flux density on the left side of the sample is significantly lower than that on the right side. However, once B_a is increased to 3.56 T, the flux density at the position of –2.5 mm increased dramatically, and the flux density on the left-hand side exceeds that on the right-hand side of the sample.

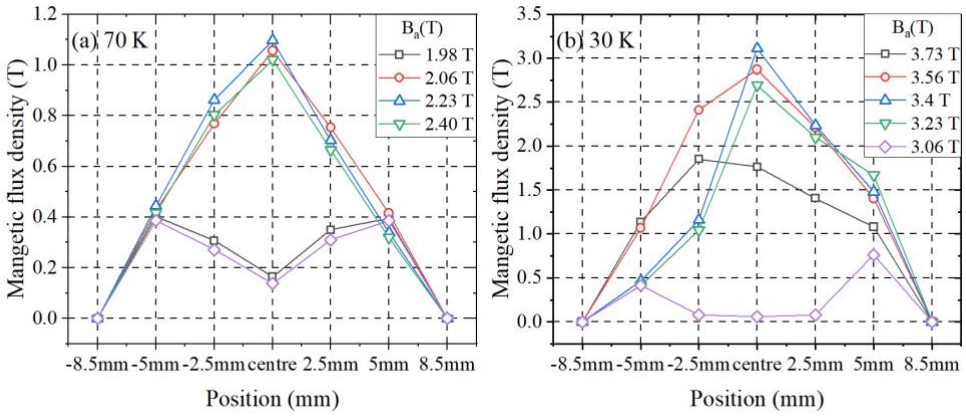

Figure 7. Trapped field profile of the YBCO bulk superconductor assembly for various applied fields B_a at (a) 70 K and (b) 30 K.

Figure 8 shows the detailed flux motion during the PFM process. For B_a = 3.40 T, flux jumps occur in the right-hand side of the sample (the green and purple curves), and the magnetic flux is pushed to the center of the assembly. For B_a = 3.56 T, flux jumps occur in the left-hand side of the sample [figure 8(b)]. It should be noted that, compared with the single bulk case, B_a = 3.40 T is insufficient to trigger a flux jump and the flux jumps occur initially in the left-hand side of the sample. A peak trapped field of 3.11 T is achieved in the bulk assembly for a B_a of only 3.40 T. The magnetization efficiency (B_T/B_a) is more than 90%. It is considered that this difference is due mainly to the presence of the adjacent neighboring sample.

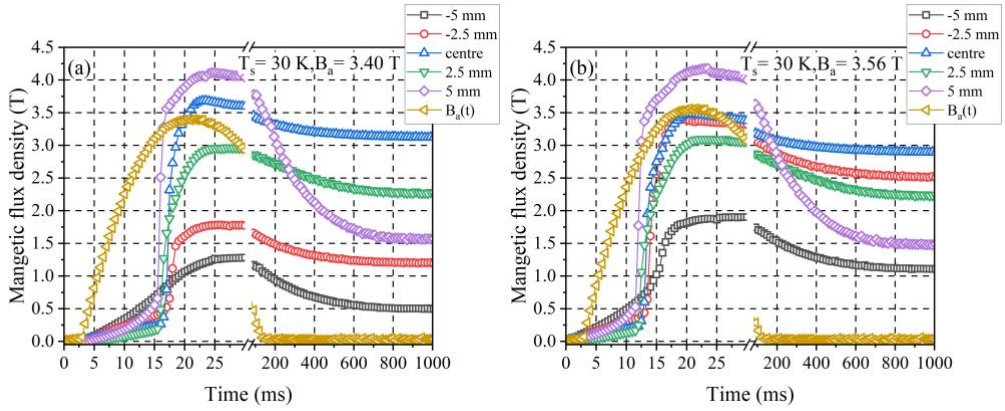

Figure 8. The dynamic variation of the measured magnetic flux density for the YBCO bulk superconductor assembly for different positions at 30 K for (a) B_a = 3.40 T and (b) B_a = 3.56 T.

A 3D numerical model was constructed (as detailed in Section 2.1) to simulate the PFM of the bulk single grain assembly in order to gain a better understanding of the flux penetration behavior.

Figure 9 shows the simulated magnetic flux density and temperature distribution of the two-sample assembly when the applied field is 4.5 T. The magnetic flux density at the junction of the two samples is 4.8 T when the applied field reaches a peak value of 4.5 T (after 20 ms). Due to the shielding currents induced during the PFM process, it can be seen that the magnetic flux is concentrated in the area of the junction, leading to an enhanced local trapped flux density. This phenomenon is similar to the magnetic lens effect reported previously [44, 45]. Therefore, the flux density at the inner edges of the samples, where they meet, attains the critical B_J value first, and is the most likely site of the first flux jump [23]. This results simultaneously in a local increase in temperature resulting in the critical temperature T_c to be exceeded at t = 15 ms, reducing significantly the local shielding capability of the assembly at this point. As a result, the flux is more likely to penetrate the assembly at the junction of the bulk single grains, accompanied by the generation of further heat. The temperature falls below the critical temperature at t = 20 ms and the shielding capacity is re-established, which explains the results shown in Figure 8. As a result, the applied magnetic field required to trigger the flux jump and obtain the maximum trapped field is reduced significantly for the bulk single grain assembly, resulting in an improved magnetization efficiency.

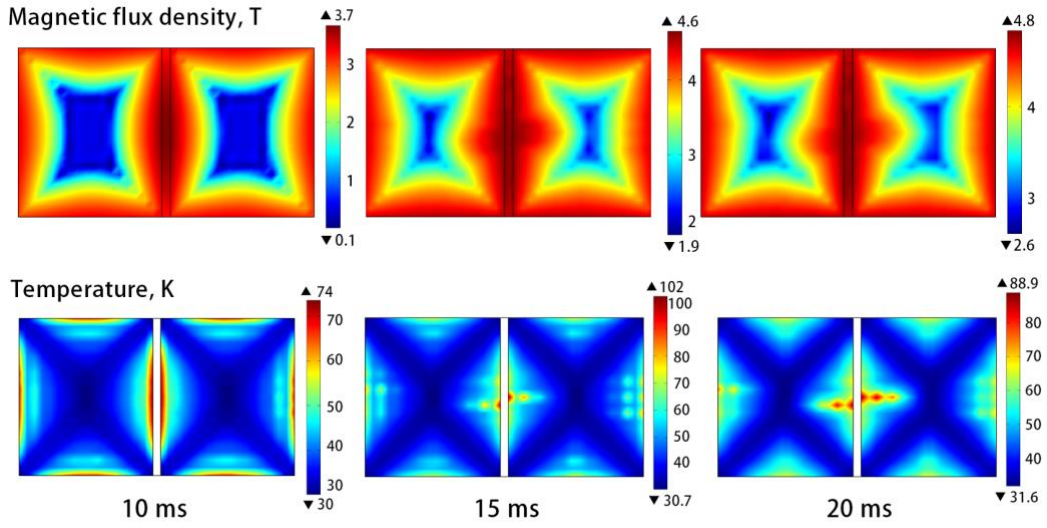

Figure 9. Simulated magnetic flux density and temperature distribution of the bulk single grain assembly at times of 10, 15 and 20 ms. (B_a = 4.5 T)

Figure 10 (a) shows the dependence of the peak trapped field on the applied field at various temperatures for the bulk single grain assembly. Unlike that obtained for the single grain sample, the optimum applied field B_{op} for the bulk assembly at 30 K is even smaller than that measured at 50 K. This can be attributed to the coupling effect that becomes more significant at the lower temperature. Figure 10(b) compares the temperature-dependent critical applied field required to trigger a flux jump in the single grain sample and in the bulk assembly. As a result of the coupling effect, the critical magnetic field B_J of the bulk assembly is significantly lower than that of a single grain. In other words, the coupling of the bulk assembly can reduce the critical magnetic field B_J required to trigger a flux jump and potentially enhance the efficiency of the PFM process.

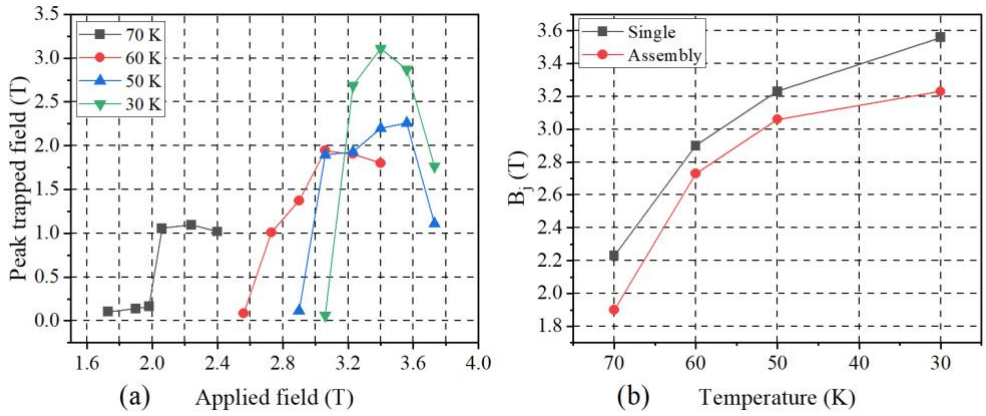

Figure 10. (a) Applied pulsed field (B_a) dependence of the peak trapped field at temperatures of 30, 50,60 and 70 K for the bulk assembly. (b) Critical field B_J required to trigger the flux jump obtained at different temperatures.

3.3. Two-step PFM

In order to maximize the trapped field, and especially the trapped field of the bulk assembly, a two-step, multi-pulse magnetization technique (MPFM) was also investigated[46]. This consists of a two-stage cooling and pulse application procedure [38]. The 1st pulse was applied at 70 K, as shown in Figure 11. B_a = 2.06 T and 1.90 T were chosen for the single sample and the bulk assembly, respectively, to allow an M-shaped trapped field distribution to be obtained initially [47]. A 2nd pulse was then applied after cooling to 30 K. Due to the residual field trapped from the 1st pulse, the optimal applied field B_{op} is enhanced from 3.73 T to 4.23 T for the bulk single grain and from 3.56 T to 4.06 T for the bulk sample assembly. The maximum trapped field with the MPFM method increases from 3.02 T to 3.39 T for the single grain and from 3.11 T to 3.31 T for the bulk assembly.

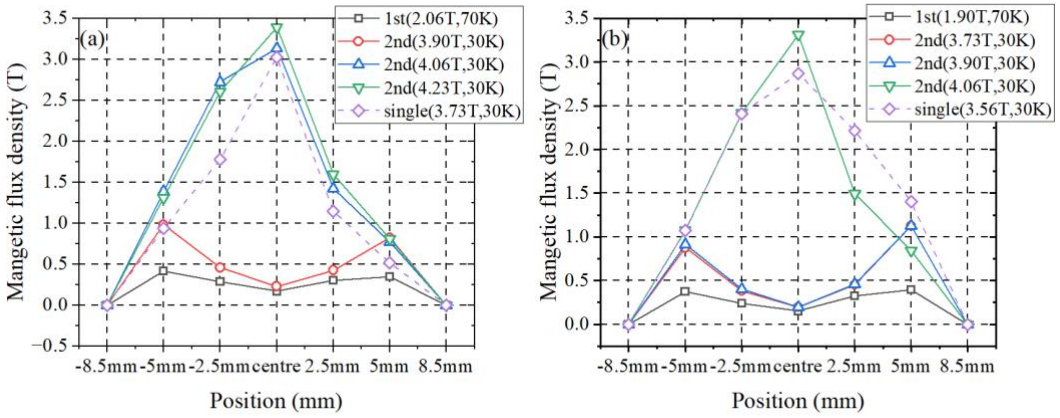

Figure 11. Trapped field profiles achieved by MPFM with temperature combinations of 70 K and 30 K(a) the bulk single grain and (b) the bulk assembly. [The purple dotted line shows equivalent data for a single applied pulse taken from Figure 4(b) and Figure 7(b) for reference].

4. Conclusions

Pulsed field magnetization (PFM) experiments have been performed on a rectangular YBCO bulk single grain and an assembly of two single grain bulk samples at temperatures of 30, 50, 60 and 70 K. The results were used to analyse the dynamic variation of the measured magnetic flux

density and the final trapped field profile for both sample arrangements. A 3D numerical model was constructed to simulate the experimental process. On this basis, it was found that the coupling of the individual bulk superconductors in the assembly enhances significantly the shielding effect at the periphery of the arrangement, but that flux penetrates at the junction of the bulk samples, resulting in an increase in local magnetic field in this region. As a result, a flux jump is more likely to occur at the junction of the two single grain samples. This promotes magnetic flux penetration and improves the magnetization efficiency from 80% to 90% at 30 K. Finally, by using a two-step, multi-pulse magnetization technique, the maximum trapped field was increased from 3.02 T to 3.39 T in a single grain bulk sample and 3.11 T to 3.31 T in a bulk, 2-sample single grain assembly. In conclusion, in addition to improving the peak trapped field obtained for single pulse, the coupling effect of bulk single grain assembly can reduce significantly the magnitude of the applied field required during PFM and therefore increase the magnetization efficiency, which has important implications for practical applications of bulk YBCO single grains in a range of electrical and magnetic devices.

Acknowledgments

This work was supported in part by the Strategic Priority Research Program of the Chinese Academy of Sciences, Grant No. XDB25000000, National Natural Science Foundation (52172271), the National Key R&D Program of China No. 2022YFE03150200, Shanghai Science and Technology Innovation Program（22511100200）.

REFERENCES

[1] J. H. Durrell *et al.*, "A trapped field of 17.6 T in melt-processed, bulk Gd-Ba-Cu-O reinforced with shrink-fit steel," *Superconductor Science and Technology,* vol. 27, no. 8, p. 082001, 2014.

[2] S. Nariki, N. Sakai, and M. Murakami, "Melt-processed Gd–Ba–Cu–O superconductor with trapped field of 3 T at 77 K," *Superconductor Science and Technology,* vol. 18, no. 2, p. S126, 2004.

[3] M. Tomita and M. Murakami, "High-temperature superconductor bulk magnets that can trap magnetic fields of over 17 tesla at 29 K," *Nature,* vol. 421, no. 6922, pp. 517-520, 2003.

[4] U. Mizutani, T. Oka, Y. Itoh, Y. Yanagi, M. Yoshikawa, and H. Ikuta, "Pulsed-field magnetization applied to high-Tc superconductors," *Applied Superconductivity,* vol. 6, no. 2-5, pp. 235-246, 1998.

[5] E. Krasnoperov, V. Korotkov, and A. Kartamyshev, "Magnetization of superconducting rings by long-duration pulses," *Technical Physics Letters,* vol. 43, no. 10, pp. 882-884, 2017.

[6] R. Shiraishi, K. Fujiyama, and H. Ohsaki, "Macroscopic magnetic flux motion in Y-Ba-Cu-O bulk superconductor during pulsed field magnetization," *IEEE transactions on applied superconductivity,* vol. 15, no. 2, pp. 3153-3156, 2005.

[7] D. Zhou *et al.*, "A portable magnetic field of> 3 T generated by the flux jump assisted, pulsed field magnetization of bulk superconductors," *Applied physics letters,* vol. 110, no. 6, p. 062601, 2017.

[8] C. P. Bean, "Magnetization of hard superconductors," *Physical review letters,* vol. 8, no. 6, p. 250, 1962.

[9] C. P. Bean, "Magnetization of high-field superconductors," *Reviews of modern physics,* vol. 36, no. 1, p. 31, 1964.

[10] R. Weinstein, D. Parks, R.-P. Sawh, K. Carpenter, and K. Davey, "A significant advantage for trapped field magnet applications—A failure of the critical state model," *Applied Physics Letters,* vol. 107, no. 15, p. 152601, 2015.

[11] M. N. Wilson, "Superconducting magnets," 1983.

[12] H. Fujishiro, T. Hiyama, T. Naito, Y. Yanagi, and Y. Itoh, "Enhancement of trapped field and total trapped flux on GdBaCuO bulk by the MMPSC+ IMRA method," *Superconductor Science and Technology,* vol. 22, no. 9, p. 095006, 2009.

[13] H. Fujishiro, T. Tateiwa, A. Fujiwara, T. Oka, and H. Hayashi, "Higher trapped field over 5 T on HTSC bulk by modified pulse field magnetizing," *Physica C: Superconductivity and its applications,* vol. 445, pp. 334-338, 2006.

[14] R. Weinstein, D. Parks, R.-P. Sawh, and K. Davey, "A phenomenon in bulk HTS that leads to greatly expanded applicability to electromechanical devices," *Journal of Applied Physics,* vol. 126, no. 22, p. 223902, 2019.

[15] V. Chabanenko *et al.*, "Magnetothermal instabilities in type II superconductors: The influence of magnetic irreversibility," *Journal of Applied Physics,* vol. 88, no. 10, pp. 5875-5883, 2000.

[16] S. Wipf, "Magnetic instabilities in type-II superconductors," *Physical Review,* vol. 161, no. 2, p. 404, 1967.

[17] V. Korotkov, E. Krasnoperov, and A. Kartamyshev, "Flux jumps at pulsed field magnetization," *Journal of Superconductivity and Novel Magnetism,* vol. 29, no. 7, pp. 1893-1896, 2016.

[18] A. Moroz, V. Kashurnikov, I. Rudnev, and A. Maksimova, "Thermal behavior of flux jumps and influence of pulse-shape on the trapped field during pulsed magnetization of a high-temperature superconductor," *Journal of Physics: Condensed Matter,* vol. 33, no. 35, p. 355901, 2021.

[19] H. Fujishiro, H. Mochizuki, T. Naito, M. Ainslie, and G. Giunchi, "Flux jumps in high-Jc MgB2 bulks during pulsed field magnetization," *Superconductor Science and Technology,* vol. 29, no. 3, p. 034006, 2016.

[20] R. Mints and A. Rakhmanov, "Critical state stability in type-II superconductors and superconducting-normal-metal composites," *Reviews of Modern Physics,* vol. 53, no. 3, p. 551, 1981.

[21] M. Ainslie, D. Zhou, H. Fujishiro, K. Takahashi, Y. Shi, and J. Durrell, "Flux jump-assisted pulsed field magnetisation of high-Jc bulk high-temperature superconductors," *Superconductor Science and Technology,* vol. 29, no. 12, p. 124004, 2016.

[22] D. Zhou *et al.*, "Exploiting flux jumps for pulsed field magnetisation," *Superconductor Science and Technology,* vol. 31, no. 10, p. 105005, 2018.

[23] D. Zhou *et al.*, "Reliable 4.8 T trapped magnetic fields in Gd–Ba–Cu–O bulk superconductors using pulsed field magnetization," *Superconductor Science and Technology,* vol. 34, no. 3, p. 034002, 2021.

[24] F. Laviano, "Vortex avalanches in superconductors visualized by magneto-optical imaging," in *Vortices and Nanostructured Superconductors*: Springer, 2017, pp. 133-157.

[25] E. Baruch-El, M. Baziljevich, B. Y. Shapiro, T. Johansen, A. Shaulov, and Y. Yeshurun, "Dendritic flux instabilities in YB a 2 C u 3 O 7− x films: Effects of temperature and magnetic field ramp rate," *Physical Review B,* vol. 94, no. 5, p. 054509, 2016.

[26] L. Li, L. Jiang, Y.-H. Zhou, A. V. Silhanek, and C. Xue, "Tunable magnetic flux avalanches triggered by a focalized laser spot," *Superconductor Science and Technology,* vol. 35, no. 8, p. 085002, 2022.

[27] Y.-H. Zhou, C. Wang, C. Liu, H. Yong, and X. Zhang, "Optically Triggered Chaotic Vortex Avalanches in Superconducting Y Ba 2 Cu 3 O 7− x Films," *Physical Review Applied,* vol. 13, no. 2, p. 024036, 2020.

[28] J.-q. Tang, G. Liu, and J.-c. Fang, "Superconducting energy storage flywheel—An attractive technology for energy storage," *Journal of Shanghai Jiaotong University (Science),* vol. 15, no. 1, pp. 76-83, 2010.

[29] M. Zhang, W. Wang, Y. Chen, and T. Coombs, "Design methodology of HTS bulk machine for direct-driven wind generation," *IEEE transactions on applied superconductivity,* vol. 22, no. 3, pp. 5201804-5201804, 2011.

[30] T. Nishimura, T. Nakamura, Q. Li, N. Amemiya, and Y. Itoh, "Potential for torque density maximization of HTS induction/synchronous motor by use of superconducting reluctance torque," *IEEE transactions on applied superconductivity,* vol. 24, no. 3, pp. 1-4, 2013.

[31] Z. Deng *et al.*, "A high-temperature superconducting maglev-evacuated tube transport

(HTS Maglev-ETT) test system," *IEEE Transactions on Applied Superconductivity,* vol. 27, no. 6, pp. 1-8, 2017.

[32] A. Arsenault, F. Sirois, and F. Grilli, "Implementation of the H-$\phi $ formulation in COMSOL Multiphysics for simulating the magnetization of bulk superconductors and comparison with the H-formulation," *IEEE Transactions on Applied Superconductivity,* vol. 31, no. 2, pp. 1-11, 2020.

[33] B. Shen, F. Grilli, and T. Coombs, "Review of the AC loss computation for HTS using H formulation," *Superconductor Science and Technology,* vol. 33, no. 3, p. 033002, 2020.

[34] B. Shen, F. Grilli, and T. Coombs, "Overview of H-formulation: A versatile tool for modeling electromagnetics in high-temperature superconductor applications," *IEEE access,* vol. 8, pp. 100403-100414, 2020.

[35] M. D. Ainslie and H. Fujishiro, "Modelling of bulk superconductor magnetization," *Superconductor Science and Technology,* vol. 28, no. 5, p. 053002, 2015.

[36] J. Zou *et al.*, "Numerical modelling and comparison of MgB2 bulks fabricated by HIP and infiltration growth," *Superconductor Science and Technology,* vol. 28, no. 7, p. 075009, 2015.

[37] H. Fujishiro, T. Naito, and M. Oyama, "Mechanism of magnetic flux trapping on superconducting bulk magnetized by pulsed field using a vortex-type coil," *Superconductor Science and Technology,* vol. 24, no. 7, p. 075015, 2011.

[38] M. D. Ainslie *et al.*, "Toward optimization of multi-pulse, pulsed field magnetization of bulk high-temperature superconductors," *IEEE Transactions on Applied Superconductivity,* vol. 28, no. 4, pp. 1-7, 2018.

[39] M. Ainslie *et al.*, "Modelling and comparison of trapped fields in (RE) BCO bulk superconductors for activation using pulsed field magnetization," *Superconductor Science and Technology,* vol. 27, no. 6, p. 065008, 2014.

[40] M. Ainslie and H. Fujishiro, *Numerical modelling of bulk superconductor magnetisation*. IOP Publishing, 2019.

[41] K. Yokoyama, R. Igarashi, R. Togasaki, and T. Oka, "Improvement of the trapped field performance of a holed superconducting bulk magnet," *IEEE Transactions on Applied Superconductivity,* vol. 25, no. 3, pp. 1-4, 2015.

[42] Y. Yanagi, Y. Itoh, M. Yoshikawa, T. Oka, H. Ikuta, and U. Mizutani, "Pulsed field magnetization of a 36 mm diameter single-domain Sm–Ba–Cu–O bulk superconductor at 30, 35 and 77 K," *Superconductor Science and Technology,* vol. 18, no. 6, p. 839, 2005.

[43] H. Fukai, Y. Kimura, S. Nariki, N. Sakai, M. Izumi, and I. Hirabayashi, "The effect of inhomogeneous flux penetration into bulk superconductor by pulsed field magnetization," *Superconductor Science and Technology,* vol. 18, no. 9, p. 1179, 2005.

[44] S. Matsumoto, T. Asano, T. Kiyoshi, and H. Wada, "Magnetic flux concentration using YBCO hollow and solid cylinders," *IEEE transactions on applied superconductivity,* vol. 14, no. 2, pp. 1666-1669, 2004.

[45] S. Choi, T. Kiyoshi, and S. Matsumoto, "Magnetic field amplifier employing high-T c bulk superconductor," *Journal of Applied Physics,* vol. 105, no. 7, p. 07E705, 2009.

[46] H. Fujishiro, T. Tateiwa, and T. Hiyama, "Enhancement of trapped field and total trapped flux on high temperature bulk superconductor by a new pulse-field magnetization method," *Japanese Journal of Applied Physics,* vol. 46, no. 7R, p. 4108, 2007.

[47] H. Fujishiro, T. Hiyama, T. Tateiwa, Y. Yanagi, and T. Oka, "Importance of initial “M-shaped” trapped field profile in a two-stage pulse field magnetization (MMPSC) method," *Physica C: Superconductivity and its applications,* vol. 463, pp. 394-397, 2007.